Hindawi
Structural Control and Health Monitoring
Volume 2023, Article ID 6968598, 16 pages
https://doi.org/10.1155/2023/6968598

Research Article

A Smoothing EKF-UI-WDF Method for Simultaneous Identification of Structural Systems and Unknown Seismic Inputs without Direct Feedthrough

Ying Lei, Chengkai Qi, and Shiyu Wang

School of Architecture and Civil Engineering, Xiamen University, Xiamen, China

Correspondence should be addressed to Ying Lei; ylei@xmu.edu.cn

Received 18 November 2022; Revised 24 January 2023; Accepted 7 February 2023; Published 30 March 2023

Academic Editor: E. Taciroglu

It is of great significance to identify structural state-parameters and the unknown seismic inputs using partial measurements of structural acceleration responses for the rapid evaluation of structures after unknown seismic excitations. However, unknown seismic inputs do not directly appear in the observation equations of measured absolute floor accelerations of building structures, i.e., there is no direct feedthrough of unknown seismic inputs in the observation equations. Current methods for the identification of joint structural systems and unknown inputs are either inapplicable or greatly influenced by measurement noises. In this paper, a method so-called smoothing extended Kalman filter with unknown input without direct feedthrough (smoothing EKF-UI-WDF) is proposed. The identification algorithm is derived in the framework of minimum-variance unbiased estimation (MVUE), and the smoothing technique is adopted to introduce subsequent observation steps in the current identification step. Then, structural states, parameters, and unknown seismic excitations without direct feedthrough are simultaneously identified recursively with only a few steps delay, and the identification results are tolerant to measurement noises. The proposed method is verified by a numerical simulation model and a practical engineering case study. Both identification results validate the effectiveness of the proposed method for the simultaneous identification of structural systems and seismic inputs without direct feedthrough.

1. Introduction

Seismic excitation information and structural state assessment are of great significance for the rapid evaluation of structural integrity after seismic excitation [1–4]. Theoretically, ground motion information can be obtained through seismic stations or sensors installed on the structure bases, but in practice, not all structures are equipped with sensors to record ground motions due to the cost of instrumentation. Moreover, due to the influence of transmission media, even the recorded data may have large errors [5]. Therefore, in the field of structural health monitoring, unknown inputs and structural states are usually identified through observed vibration response data of structures [6–10]. However, simultaneous identification of unknown seismic excitations and corresponding structural system states using partial responses of structures is still a challenging problem, especially when the structural parameters are unknown. System identification methods based on Kalman filter (KF) and extended Kalman filter (EKF) methods have made great progress [11, 12]. Through the state and observation equations, satisfactory identification results can be obtained with model error and observation noises. Currently, there are many joint identification methods for structural systems and unknown inputs developed based on the extensions of traditional KF and EKF [13–18]. Recently, Yuen and Huang modeled the unknown input as modulated filtered white noise or modulated colored noise excitation [19–21] and using EKF combined with the Bayesian method to estimate the uncertain filter parameters to reconstruct the unknown input. But most methods still need to meet the condition that the unknown inputs directly appear in the observation equation or the so-called with direct feedthrough. It is worth noting that the

situation of unknown seismic inputs is different from that of external excitations as the monitored floor accelerations of building structures are absolute acceleration values. In this scope, the unknown seismic input terms do not directly appear in the observation equations or the so-called without direct feedthrough.

Currently, there are far fewer studies for the identification of systems without direct feedthrough. In terms of known structural parameters, Gillijns and De Moor [22] proposed a joint input-state estimation method for the system without direct feedthrough. Pan et al. [23] derived the Kalman filtering method with the global optimal solution and unknown input without direct feedthrough (KF-UI-WDF). In terms of unknown structural parameters, Wan et al. [24] extended Gillijns and De Moor's work by adding the structural parameters to the state vector. Similar to the KF-UI-WDF, Pan et al. [25] proposed the extended Kalman filter with unknown inputs without direct feedthrough (EKF-UI-WDF). The author has also proposed some methods for the identification of structural systems and unknown inputs without direct feedthrough by adopting the assumption of first-order hold (FOH) in adjacent steps for unknown inputs [26, 27]. Nevertheless, identifications are not well performed when measurement noises increase.

In essence, identification results for the system without direct feedthrough of unknown inputs are sensitive to measurement noises [28]. Some researchers proposed the offline methods, [3, 29, 30] e.g. the Tikhonov regularization and maximum a posteriori estimation (MAP) to improve the identification results. Recently, Taher et al. [3] adopted a least squares-based MAP to improve the seismic input estimation, and the estimated input is used as known input in the conventional KF method to obtain the unknown structural states. However, such offline methods cannot provide real-time identification for the earthquake-excited structures.

In the traditional filtering method, the estimation of the $(k+1)$ th step is based on the measurements from 1st step to $(k+1)$ th step. If a certain time delay is allowed for the estimation that is the estimation of the $(k+1)$ th step is based on the measurements from 1st step to $(k+N)$ th $(N>1)$ step. In this way, the measurements from $(k+2)$ th step to $(k+N)$ th step is the added observation information compared to traditional methods. This addition improves the quality of the estimation at the current step since the addition is from the later steps. Actually, such a technique is the so-called smoothing that has been adopted by researchers [28, 31–35]. Recently, Ebrahimzadeh et al. [35] proposed a method for joint identification of structural state and unknown inputs by combining smoothing technique, but structural parameters need to be known prior. Maes et al. [31] proposed a method of joint identification of input, state and parameter by combining smoothing and a two-step filtering for linear structural systems.

In this paper, a smoothing EKF-UI-WDF method is proposed in the framework of minimum-variance unbiased estimation (MVUE) to identify structural systems and unknown inputs without direct feedthrough. The main contributions of this paper include: (1) structural states, parameters of the structural systems and the unknown inputs without direct feedthrough can be simultaneously identified, and the identification is tolerant to the measurement noises supported by the smoothing technique; (2) compared with current offline identification methods, real-time identification is less sacrificed in the proposed method, which better meets the requirements of rapid evaluation and timely warning under seismic conditions. The validation of the proposed method in this paper includes a numerical example and a real-world application. Different observation situations, displacements for numerical example and absolute accelerations for real-world structure, which both lead to the systems and unknown inputs without direct feedthrough, are used to validate the proposed method.

2. The Proposed Smoothing EKF-UI-WDF Method

The proposed smoothing EKF-UI-WDF method is derived under the framework of MVUE in state-space by combing the smoothing scheme.

2.1. Structural State and Observation Equations. The equation of motion of an earthquake-excited structure with n DOFs can be formulated as:

$$\mathbf{M}\ddot{\mathbf{x}} + \mathbf{F}(\mathbf{x}, \dot{\mathbf{x}}, \boldsymbol{\theta}) = -\mathbf{M}\mathbf{L}\ddot{x}_g, \tag{1}$$

where $\mathbf{M}$ is structural mass matrix, $\mathbf{F}(\mathbf{x}, \dot{\mathbf{x}}, \theta)$ is structural restoring force vector, $\mathbf{x}, \dot{\mathbf{x}}, \ddot{\mathbf{x}}$ denote the vectors of structural displacement, velocity and acceleration, respectively. θ denotes unknown structural parameters, e.g. stiffness, damping ratio and nonlinear parameters, $\mathbf{L}$ is the influence vector of seismic input, and $\ddot{x}_g$ represents the unknown seismic acceleration.

Let structural state vector $\mathbf{Z} = [\mathbf{x}^T, \dot{\mathbf{x}}^T, \theta^T]^T$, equation (1) can be converted into the state-space as follow:

$$\dot{\mathbf{Z}} = \begin{bmatrix} \dot{\mathbf{x}} \\ -\mathbf{M}^{-1}\mathbf{F}(\mathbf{x}, \dot{\mathbf{x}}, \boldsymbol{\theta}) - \mathbf{L}\ddot{x}_g \quad \mathbf{0} \end{bmatrix} = \mathbf{g}(\mathbf{Z}) + \mathbf{B}^u\ddot{x}_g, \tag{2}$$

where $\mathbf{g}(\mathbf{Z}) = \begin{bmatrix} \dot{\mathbf{x}}^T & (-\mathbf{M}^{-1}\mathbf{F}(\mathbf{x}, \dot{\mathbf{x}}, \theta))^T & \mathbf{0}^T \end{bmatrix}^T$ and $\mathbf{B}^u = \begin{bmatrix} \mathbf{0}^T & -\mathbf{L}^T & \mathbf{0}^T \end{bmatrix}^T$.

Based on the smoothing scheme, the estimation of $\mathbf{Z}_k$ can be denoted as $\hat{\mathbf{Z}}_{k|k+N-1}$, in which the subscript "$k|k+N-1$" denotes the estimation of $\mathbf{Z}_k$ given the observation sequence $\begin{bmatrix} \mathbf{y}_1^T \mathbf{y}_2^T \cdots \mathbf{y}_k^T \cdots \mathbf{y}_{k+N-1}^T \end{bmatrix}^T$. Then, based on the linearization in the EKF procedure, equation (2) is linearized as:

$$\begin{aligned} \dot{\mathbf{Z}} &= \mathbf{g}(\mathbf{Z}) + \mathbf{B}^u\ddot{x}_g \approx \mathbf{g}\left(\hat{\mathbf{Z}}_{k|k+N-1}\right) + \mathbf{U}_k\left(\mathbf{Z} - \hat{\mathbf{Z}}_{k|k+N-1}\right) + \mathbf{B}^u\ddot{x}_g \\ &= \mathbf{U}_k\mathbf{Z} + \mathbf{B}^u\ddot{x}_g + \mathbf{u}_k, \end{aligned} \tag{3}$$

where $\mathbf{U}_k = \partial\mathbf{g}(\mathbf{Z})/\partial\mathbf{Z}^T|_{\mathbf{Z}=\hat{\mathbf{Z}}_{k|k+N-1}}$ and $\mathbf{u}_k = \mathbf{g}(\hat{\mathbf{Z}}_{k|k+N-1}) - \mathbf{U}_k\hat{\mathbf{Z}}_{k|k+N-1}$.

Then, equation (3) can be discretized as:

$$\mathbf{Z}_{k+1} = \mathbf{A}_k\mathbf{Z}_k + \mathbf{B}_k\ddot{x}_g + \mathbf{g}_k + \mathbf{w}_k, \tag{4}$$

in which, $\mathbf{A}_k = \mathbf{e}^{\mathbf{U}_k\Delta t}$, $\mathbf{B}_k = (\mathbf{A}_k - \mathbf{I})(\mathbf{U}_k)^{-1}\mathbf{B}^u$, $\mathbf{g}_k = (\mathbf{A}_k - \mathbf{I})(\mathbf{U}_k)^{-1}\mathbf{u}_k$, Δt is the sampling interval and $\mathbf{w}_k$ is the modeling error with the zero average and $\mathbf{Q}_k$ variance.

When observed responses are absolute accelerations or displacements of the earthquake-excited structure, the observation equation can be formulated as:

$$\mathbf{y}_{k+1} = \mathbf{h}(\mathbf{Z}_{k+1}) + \mathbf{v}_{k+1}, \tag{5}$$

where the function $\mathbf{h}(\mathbf{Z}_{k+1})$ is only related to the state vector, $\mathbf{v}_{k+1}$ is the measurements noises term with the zero mean value and $\mathbf{R}_k$ covariance. The determination of the values of $\mathbf{Q}_k$ and $\mathbf{R}_k$ has been investigated by some researchers [36, 37], so it is not discussed in this papers.

The expression of $\mathbf{h}(\mathbf{Z}_{k+1})$ can be written as follows according to different observations:

(1) Absolute accelerations observations ($\mathbf{y}_{k+1} = \mathbf{S}_a \ddot{\mathbf{x}}^a_{k+1}$)

$$\begin{aligned}\mathbf{h}(\mathbf{Z}_{k+1}) &= \mathbf{S}_a\left(\ddot{\mathbf{x}}_{k+1} + \mathbf{L}\ddot{x}_{g,k+1}\right)\\ &= -\mathbf{S}_a\mathbf{M}^{-1}\mathbf{F}(\mathbf{x}_{k+1}, \dot{\mathbf{x}}_{k+1}, \boldsymbol{\theta}_{k+1}).\end{aligned} \tag{6}$$

(2) Displacements observations ($\mathbf{y}_{k+1} = \mathbf{S}_d \mathbf{x}_{k+1}$)

$$\mathbf{h}(\mathbf{Z}_{k+1}) = \mathbf{S}_d \mathbf{x}_{k+1}. \tag{7}$$

If equation (5) is a nonlinear function, it is linearized by Taylor expansion at the defined point $\widehat{\mathbf{Z}}_{k+1|k+N-1}$,

$$\widehat{\mathbf{Z}}_{k+1|k+N-1} = \widehat{\mathbf{Z}}_{k|k+N-1} + \int_{k\Delta t}^{(k+1)\Delta t}\left[\mathbf{g}\left(\widehat{\mathbf{Z}}_{t|k+N-1}\right)\right]\mathrm{d}t + \mathbf{B}_k\widehat{\ddot{x}}_{g,k-1|k+N-1}, \tag{8}$$

where $\widehat{\ddot{x}}_{g,k-1|k+N-1}$ is the estimation of the $\ddot{x}_{g,k-1}$. Then, the linearized observation equation is derived as:

$$\begin{aligned}&\mathbf{y}_{k+1} = \mathbf{h}(\mathbf{Z}_{k+1}) + \mathbf{v}_{k+1} \approx \mathbf{h}\left(\widehat{\mathbf{Z}}_{k+1|k+N-1}\right) + \mathbf{H}_{k+1}\left(\mathbf{Z}_{k+1} - \widehat{\mathbf{Z}}_{k+1|k+N-1}\right) + \mathbf{v}_{k+1} = \mathbf{H}_{k+1}\mathbf{Z}_{k+1} + \mathbf{h}_{k+1} + \mathbf{v}_{k+1},\\ &\mathbf{H}_{k+1} = \left.\frac{\partial \mathbf{h}(\mathbf{Z}_{k+1})}{\partial \mathbf{Z}^T_{k+1}}\right|_{\mathbf{Z}_{k+1}=\widehat{\mathbf{Z}}_{k+1|k+N-1}},\\ &\mathbf{h}_{k+1,k+1} = \mathbf{h}\left(\widehat{\mathbf{Z}}_{k+1|k+N-1}\right) - \mathbf{H}_{k+1}\widehat{\mathbf{Z}}_{k+1|k+N-1}\end{aligned} \tag{9}$$

According to the smoothing scheme [31], a new expanded observation equation can be derived as:

$$\mathbf{Y}_{k+1} = \overline{\mathbf{H}}_{k+1}\mathbf{Z}_{k+1} + \overline{\mathbf{D}}_{k+1}\mathbf{F}^{\mathbf{u}}_{k+1} + \overline{\mathbf{L}}_{k+1}\overline{\mathbf{g}}_{k+1} + \overline{\mathbf{L}}_{k+1}\mathbf{W}_{k+1} + \overline{\mathbf{h}}_{k+1} + \mathbf{V}_{k+1}, \tag{10}$$

in which,

$$\begin{aligned}&\mathbf{Y}_{k+1} = \begin{bmatrix}\mathbf{y}_{k+1}\\ \mathbf{y}_{k+2}\\ \vdots\\ \mathbf{y}_{k+N}\end{bmatrix}; \overline{\mathbf{H}}_{k+1} = \begin{bmatrix}\mathbf{H}_{k+1}\\ \mathbf{H}_{k+1}\mathbf{A}_k\\ \vdots\\ \mathbf{H}_{k+1}\mathbf{A}_k^{N-1}\end{bmatrix}; \overline{\mathbf{D}}_{k+1} = \begin{bmatrix}0 & 0 & \cdots & 0\\ 0 & \mathbf{H}_{k+1}\mathbf{B}_k & \cdots & 0\\ \vdots & \vdots & \ddots & \vdots\\ 0 & \mathbf{H}_{k+1}\mathbf{A}_k^{N-1}\mathbf{B}_k & \cdots & \mathbf{H}_{k+1}\mathbf{B}_k\end{bmatrix}; \mathbf{F}^{u}_{k+1} = \left[\ddot{x}_{g,k}\ \ddot{x}_{g,k+1}\ \vdots\ \ddot{x}_{g,k+N-1}\right];\\ &\overline{\mathbf{L}}_{k+1} = \begin{bmatrix}0 & 0 & \cdots & 0\\ 0 & \mathbf{H}_{k+1} & \cdots & 0\\ \vdots & \vdots & \ddots & \vdots\\ 0 & \mathbf{H}_{k+1}\mathbf{A}_k^{N-1} & \cdots & \mathbf{H}_{k+1}\end{bmatrix}; \overline{\mathbf{g}}_{k+1} = \begin{bmatrix}\mathbf{g}_k\\ \mathbf{g}_k\\ \vdots\\ \mathbf{g}_k\end{bmatrix}; \overline{\mathbf{h}}_{k+1} = \begin{bmatrix}\mathbf{h}_{k+1}\\ \mathbf{h}_{k+1}\\ \vdots\\ \mathbf{h}_{k+1}\end{bmatrix}; \mathbf{W}_{k+1} = \begin{bmatrix}\mathbf{w}_k\\ \mathbf{w}_{k+1}\\ \vdots\\ \mathbf{w}_{k+N-1}\end{bmatrix}; \mathbf{V}_{k+1} = \begin{bmatrix}\mathbf{v}_{k+1}\\ \mathbf{v}_{k+2}\\ \vdots\\ \mathbf{v}_{k+N}\end{bmatrix}.\end{aligned} \tag{11}$$

2.2. Joint Input-State-Parameter Estimation

2.2.1. Recursive Filter. The proposed method aims to simultaneously identify the unknown seismic input and structural system based on the derived state equation (4) and the observation equation (10).

First, the state $\breve{\mathbf{Z}}_{k+1|k+N-1}$ is defined as

$$\breve{\mathbf{Z}}_{k+1|k+N-1} \triangleq \mathbf{A}_k \hat{\mathbf{Z}}_{k|k+N-1} + \mathbf{g}_k. \tag{12}$$

Based on equation (10), the input estimation is given by

$$\hat{\mathbf{F}}^u_{k+1|k+N} = \mathbf{M}_{k+1}\left(\mathbf{Y}_{k+1} - \overline{\mathbf{H}}_{k+1}\breve{\mathbf{Z}}_{k+1|k+N-1} - \overline{\mathbf{L}}_{k+1}\overline{\mathbf{g}}_{k+1} - \overline{\mathbf{h}}_{k+1}\right), \tag{13}$$

where $\mathbf{M}_{k+1}$ is the input gain matrix to be solved.

According to the relationship between $\ddot{x}_{g,k}$ and $\mathbf{F}^u_{k+1}$ in equation (11), one can obtain the transfer equation by defining $\mathbf{I}_F \triangleq [\,1 \;\; \mathbf{0}\,]$.

$$\hat{\ddot{x}}_{g,k|k+N} = \mathbf{I}_F \hat{\mathbf{F}}^u_{k+1|k+N}. \tag{14}$$

Also, the predicted state $\tilde{\mathbf{Z}}_{k+1|k+N-1}$ is given based on equation (4) as:

$$\tilde{\mathbf{Z}}_{k+1|k+N-1} = \mathbf{A}_k \hat{\mathbf{Z}}_{k|k+N-1} + \mathbf{B}_k \hat{\ddot{x}}_{g,k|k+N} + \mathbf{g}_k. \tag{15}$$

Then, the estimated state $\hat{\mathbf{Z}}_{k+1|k+N}$ can be obtained by updating the $\tilde{\mathbf{Z}}_{k+1|k+N-1}$ with equation (10):

$$\hat{\mathbf{Z}}_{k+1|k+N} = \tilde{\mathbf{Z}}_{k+1|k+N-1} + \mathbf{K}_{k+1}\left(\mathbf{Y}_{k+1} - \overline{\mathbf{H}}_{k+1}\tilde{\mathbf{Z}}_{k+1|k+N-1} - \overline{\mathbf{D}}_{k+1}\hat{\mathbf{F}}^u_{k+1|k+N} - \overline{\mathbf{L}}_{k+1}\overline{\mathbf{g}}_{k+1} - \overline{\mathbf{h}}_{k+1}\right), \tag{16}$$

where $\mathbf{K}_{k+1}$ is the state gain matrix to be solved.

Equations (12)–(16) are the adopted forms of the recursive filter, in which the unknown gain matrices $\mathbf{M}_{k+1}$ and $\mathbf{K}_{k+1}$ is estimated in the framework of minimum-variance unbiased estimation (MVUE).

2.2.2. Input Estimation

(1) Unbiadeness Condition. Based on the equation (13), one can define

$$\mathbf{e}^{\mathbf{Y}}_{k+1} \triangleq \mathbf{Y}_{k+1} - \overline{\mathbf{H}}_{k+1}\breve{\mathbf{Z}}_{k+1|k+N-1} - \overline{\mathbf{L}}_{k+1}\overline{\mathbf{g}}_{k+1} - \overline{\mathbf{h}}_{k+1}. \tag{17}$$

By substituting equation (4) into equation (10) and using equations (12) and (17) can be derived as follows:

$$\mathbf{e}^{\mathbf{Y}}_{k+1} = \overline{\mathbf{D}}_{k+1}\mathbf{F}^{\mathbf{u}}_{k+1} + \overline{\mathbf{H}}_{k+1}\mathbf{B}_k\mathbf{f}^u_k + \overline{\mathbf{H}}_{k+1}\mathbf{A}_k\hat{\mathbf{e}}^{\mathbf{Z}}_k + \overline{\mathbf{H}}_{k+1}\mathbf{w}_k + \overline{\mathbf{L}}_{k+1}\mathbf{W}_{k+1} + \mathbf{V}_{k+1}, \tag{18}$$

where the estimated error of the state is denoted as $\hat{\mathbf{e}}^{\mathbf{Z}}_k \triangleq \mathbf{Z}_k - \hat{\mathbf{Z}}_{k|k+N-1}$.

Based on the relationship between $\mathbf{w}_k$ and $\mathbf{W}_{k+1}$ in equation (11), it is derived:

$$\mathbf{w}_k = \mathbf{I}_W \mathbf{W}_{k+1}, \tag{19}$$

where $\mathbf{I}_W \triangleq [\,\mathbf{I} \;\; \mathbf{0}\,]$.

To obtain a simpler form of equation (18), some terms are defined as:

$$\Gamma_{k+1} \triangleq \overline{\mathbf{H}}_{k+1}\mathbf{A}_k, \breve{\mathbf{L}}_{k+1} \triangleq \overline{\mathbf{L}}_{k+1} + \overline{\mathbf{H}}_{k+1}\mathbf{I}_W, \breve{\mathbf{D}}_{k+1} \triangleq \overline{\mathbf{D}}_{k+1} + \overline{\mathbf{H}}_{k+1}\mathbf{B}_k\mathbf{I}_F; \mathbf{e}_{k+1} \triangleq \Gamma_{k+1}\hat{\mathbf{e}}^{\mathbf{Z}}_k + \breve{\mathbf{L}}_{k+1}\mathbf{W}_{k+1} + \mathbf{V}_{k+1}. \tag{20}$$

Then, equation (18) can be rewritten as:

$$\mathbf{e}^{\mathbf{Y}}_{k+1} = \breve{\mathbf{D}}_{k+1}\mathbf{F}^u_{k+1} + \mathbf{e}_{k+1}. \tag{21}$$

One can directly get the least-square estimation (LSE) of unknown input from equation (21), however, the variance of the estimated error is not minimum.

To make estimation (equation (13)) unbiased, an unbiased condition for the input gain matrix $\mathbf{M}_{k+1}$ is derived.

According to the unbiasedness of input estimation, $E[\hat{\mathbf{F}}^u_{k+1|k+N}] = \mathbf{F}^u_{k+1}$, one can get:

$$E\left[\hat{\mathbf{F}}^u_{k+1|k+N}\right] = \mathbf{M}_{k+1}E\left[\mathbf{e}^{\mathbf{Y}}_{k+1}\right] = \mathbf{M}_{k+1}\breve{\mathbf{D}}_{k+1}\mathbf{F}^u_{k+1} = \mathbf{F}^u_{k+1}. \tag{22}$$

From equation (22), an unbiasedness condition for $\mathbf{M}_{k+1}$ is obtained:

$$\mathbf{M}_{k+1}\breve{\mathbf{D}}_{k+1} = \mathbf{I}. \tag{23}$$

(2) Minimum-Variance Condition. Furthermore, a weighted least-square estimation (WLSE) for the equation (21) is used to estimate the unknown input satisfied MVUE. By defining $\widetilde{\mathbf{R}}_{k+1} \triangleq E[(\mathbf{e}_{k+1})(\mathbf{e}_{k+1})^T]$,

$$\widetilde{\mathbf{R}}_{k+1} = \Gamma_{k+1}\widehat{\mathbf{P}}_k^{\mathbf{Z}}\Gamma_{k+1}^T + \breve{\mathbf{L}}_{k+1}\overline{\mathbf{Q}}_k\breve{\mathbf{L}}_{k+1}^T + \overline{\mathbf{R}}_{k+1} + S\left(\Gamma_{k+1}\widehat{\mathbf{P}}_k^{\mathbf{ZW}}\breve{\mathbf{L}}_{k+1}^T\right) + S\left(\Gamma_{k+1}\widehat{\mathbf{P}}_k^{\mathbf{ZV}}\right), \tag{24}$$

where

$$\overline{\mathbf{Q}}_k = E\left[(\mathbf{W}_{k+1})(\mathbf{W}_{k+1})^T\right], \overline{\mathbf{R}}_{k+1} = E\left[(\mathbf{V}_{k+1})(\mathbf{V}_{k+1})^T\right], S(\mathbf{X}) \triangleq \mathbf{X} + \mathbf{X}^T, \widehat{\mathbf{P}}_k^{\mathbf{Z}} = E\left[\left(\widehat{\mathbf{e}}_k^{\mathbf{Z}}\right)\left(\widehat{\mathbf{e}}_k^{\mathbf{Z}}\right)^T\right], \widehat{\mathbf{P}}_k^{\mathbf{ZV}} = E\left[\left(\widehat{\mathbf{e}}_k^{\mathbf{Z}}\right)(\mathbf{V}_{k+1})^T\right]. \tag{25}$$

The weighting matrix $\widetilde{\mathbf{S}}_{k+1}^{-1}$ is obtained from the non-singular matrix $\widetilde{\mathbf{S}}_{k+1}$ which satisfies $\widetilde{\mathbf{S}}_{k+1}\widetilde{\mathbf{S}}_{k+1}^T = \widetilde{\mathbf{R}}_{k+1}$. Then, a weighted form of equation (21) is formulated as:

$$\widetilde{\mathbf{S}}_{k+1}^{-1}\mathbf{e}_{k+1}^{\mathbf{Y}} = \widetilde{\mathbf{S}}_{k+1}^{-1}\breve{\mathbf{D}}_{k+1}\mathbf{F}_{k+1}^u + \widetilde{\mathbf{S}}_{k+1}^{-1}\mathbf{e}_{k+1}, \tag{26}$$

and

$$E\left[\left(\widetilde{\mathbf{S}}_{k+1}^{-1}\mathbf{e}_{k+1}\right)\right] = \mathbf{0}; E\left[\left(\widetilde{\mathbf{S}}_{k+1}^{-1}\mathbf{e}_{k+1}\right)\left(\widetilde{\mathbf{S}}_{k+1}^{-1}\mathbf{e}_{k+1}\right)^T\right] = \widetilde{\mathbf{S}}_{k+1}^{-1}E\left[(\mathbf{e}_{k+1})(\mathbf{e}_{k+1})^T\right]\widetilde{\mathbf{S}}_{k+1}^{-T} = \mathbf{I}. \tag{27}$$

The least-square estimation (LSE) of equation (26) is unbiased and has minimum-variance. So the unknown input is estimated as:

$$\widehat{\mathbf{F}}_{k+1|k+N}^u = \left(\breve{\mathbf{D}}_{k+1}^T\widetilde{\mathbf{R}}_{k+1}^{-1}\breve{\mathbf{D}}_{k+1}\right)^{-1}\breve{\mathbf{D}}_{k+1}^T\widetilde{\mathbf{R}}_{k+1}^{-1}\left(\mathbf{Y}_{k+1} - \overline{\mathbf{H}}_{k+1}\breve{\mathbf{Z}}_{k+1|k+N-1} - \overline{\mathbf{L}}_{k+1}\overline{\mathbf{g}}_{k+1} - \overline{\mathbf{h}}_{k+1}\right). \tag{28}$$

By comparing with equation (13), the input gain matrix $\mathbf{M}_{k+1}$ is obtained by the minimum-variance condition as:

$$\mathbf{M}_{k+1} = \left(\breve{\mathbf{D}}_{k+1}^T\widetilde{\mathbf{R}}_{k+1}^{-1}\breve{\mathbf{D}}_{k+1}\right)^{-1}\breve{\mathbf{D}}_{k+1}^T\widetilde{\mathbf{R}}_{k+1}^{-1}. \tag{29}$$

To check the unbiased condition, it is noted that equation (29) automatically satisfies $\mathbf{M}_{k+1}\breve{\mathbf{D}}_{k+1} = \mathbf{I}$.

2.2.3. State Estimation. The unknown state can be estimated once the state gain matrix $\mathbf{K}_{k+1}$ is estimated. Similar to the input estimation, the unbiased and minimum-variance conditions are used for the derivation of $\mathbf{K}_{k+1}$.

(1) Unbiased Condition. By defining the error of predicted state $\widetilde{\mathbf{e}}_{k+1}^{\mathbf{Z}} \triangleq \mathbf{Z}_{k+1} - \widetilde{\mathbf{Z}}_{k+1|k+N-1}$ and error of estimated input $\widehat{\mathbf{e}}_k^{\mathbf{f}} \triangleq \ddot{x}_{g,k} - \widehat{\ddot{x}}_{g,k|k+N}$, the error of estimated state $\widehat{\mathbf{e}}_{k+1}^{\mathbf{Z}} = \mathbf{Z}_{k+1} - \widehat{\mathbf{Z}}_{k+1|k+N}$ can be derived based on equations (4) and (15) as:

$$\widetilde{\mathbf{e}}_{k+1}^{\mathbf{Z}} = \mathbf{A}_k\widehat{\mathbf{e}}_k^{\mathbf{Z}} + \mathbf{B}_k\widehat{\mathbf{e}}_k^{\mathbf{f}} + \mathbf{w}_k. \tag{30}$$

Also, by defining the error $\widehat{\mathbf{e}}_{k+1}^{\mathbf{F}} \triangleq \mathbf{F}_{k+1}^u - \widehat{\mathbf{F}}_{k+1|k+N}^u$, the estimated error $\widehat{\mathbf{e}}_k^{\mathbf{f}}$ can be derived from equations (13), (14) and (21) as:

$$\widehat{\mathbf{e}}_k^{\mathbf{f}} = \mathbf{I}_F\widehat{\mathbf{e}}_{k+1}^{\mathbf{F}} = -\mathbf{I}_F\mathbf{M}_{k+1}\mathbf{e}_{k+1} = -\mathbf{I}_F\mathbf{M}_{k+1}\left(\Gamma_{k+1}\widehat{\mathbf{e}}_k^{\mathbf{Z}} + \breve{\mathbf{L}}_{k+1}\mathbf{W}_{k+1} + \mathbf{V}_{k+1}\right). \tag{31}$$

With some terms defined as $\mathbf{G}_{k+1} \triangleq \mathbf{B}_k\mathbf{I}_F\mathbf{M}_{k+1}$, $\mathbf{J}_{k+1} \triangleq -\mathbf{G}_{k+1}\breve{\mathbf{L}}_{k+1} + \mathbf{I}_W$, $\mathbf{A}_k^* \triangleq \mathbf{A}_k - \mathbf{G}_{k+1}\Gamma_{k+1}$ and $\mathbf{w}_k^* \triangleq \mathbf{J}_{k+1}\mathbf{W}_{k+1} - \mathbf{G}_{k+1}\mathbf{V}_{k+1}$, a simple form of equation (30) can be derived by substituting equation (31) into equation (30) as:

$$\tilde{\mathbf{e}}_{k+1}^{\mathbf{Z}} = \mathbf{A}_k^*\hat{\mathbf{e}}_k^{\mathbf{Z}} + \mathbf{w}_k^*. \tag{32}$$

Then, the explicit function between $\hat{\mathbf{e}}_{k+1}^{\mathbf{Z}}$ and $\hat{\mathbf{e}}_k^{\mathbf{Z}}$ can be established by using equations (4), (16) and (32):

$$\hat{\mathbf{e}}_{k+1}^{\mathbf{Z}} = \tilde{\mathbf{e}}_{k+1}^{\mathbf{Z}} - \mathbf{K}_{k+1}\left(\mathbf{I} - \breve{\mathbf{D}}_{k+1}\mathbf{M}_{k+1}\right)\mathbf{e}_{k+1} = \hat{\mathbf{A}}_{k+1}\hat{\mathbf{e}}_k^{\mathbf{Z}} + \hat{\mathbf{J}}_{k+1}\mathbf{W}_{k+1} + \hat{\mathbf{G}}_{k+1}\mathbf{V}_{k+1}, \tag{33}$$

where

$$\begin{aligned}&\hat{\mathbf{A}}_{k+1} \triangleq \mathbf{A}_k^* - \boldsymbol{\Phi}_{k+1}\Gamma_{k+1}, \hat{\mathbf{J}}_{k+1} \triangleq \mathbf{J}_{k+1} - \boldsymbol{\Phi}_{k+1}\breve{\mathbf{L}}_{k+1}, \hat{\mathbf{G}}_{k+1} \triangleq -\mathbf{G}_{k+1} - \boldsymbol{\Phi}_{k+1},\\ &\boldsymbol{\Phi}_{k+1} \triangleq \mathbf{K}_{k+1}\left(\mathbf{I} - \breve{\mathbf{D}}_{k+1}\mathbf{M}_{k+1}\right).\end{aligned} \tag{34}$$

For the unbiased condition $E[\hat{\mathbf{e}}_{k+1}^{\mathbf{Z}}] = \mathbf{0}$, it is derived that

$$E\left[\hat{\mathbf{e}}_{k+1}^{\mathbf{Z}}\right] = E\left[\hat{\mathbf{A}}_{k+1}\hat{\mathbf{e}}_k^{\mathbf{Z}} + \hat{\mathbf{J}}_{k+1}\mathbf{W}_{k+1} + \hat{\mathbf{G}}_{k+1}\mathbf{V}_{k+1}\right] = \hat{\mathbf{A}}_{k+1}E\left[\hat{\mathbf{e}}_k^{\mathbf{Z}}\right]. \tag{35}$$

From equation (35), it is found that any value of $\mathbf{K}_{k+1}$ is acceptable for the unbiased condition once $\hat{\mathbf{Z}}_{k|k+N-1}$ is unbiased, i.e., $(E[\hat{\mathbf{e}}_k^{\mathbf{Z}}] = \mathbf{0})$.

(2) Minimum-Variance Condition. From equation (33), the variance $\hat{\mathbf{P}}_{k+1}^{\mathbf{Z}} = E[(\hat{\mathbf{e}}_{k+1}^{\mathbf{Z}})(\hat{\mathbf{e}}_{k+1}^{\mathbf{Z}})^T]$ is derived as:

$$\hat{\mathbf{P}}_{k+1}^{\mathbf{Z}} = \mathbf{K}_{k+1}\boldsymbol{\Psi}_{k+1}\mathbf{K}_{k+1}^T + S\left(\mathbf{K}_{k+1}\Upsilon_{k+1}\right) + \tilde{\mathbf{P}}_{k+1}^{\mathbf{Z}}, \tag{36}$$

where

$$\begin{aligned}&\boldsymbol{\Psi}_{k+1} \triangleq E\left[\left(\left(\mathbf{I} - \breve{\mathbf{D}}_{k+1}\mathbf{M}_{k+1}\right)\mathbf{e}_{k+1}\right)\left(\left(\mathbf{I} - \breve{\mathbf{D}}_{k+1}\mathbf{M}_{k+1}\right)\mathbf{e}_{k+1}\right)^T\right] = \left(\mathbf{I} - \breve{\mathbf{D}}_{k+1}\mathbf{M}_{k+1}\right)\tilde{\mathbf{R}}_{k+1}\left(\mathbf{I} - \breve{\mathbf{D}}_{k+1}\mathbf{M}_{k+1}\right)^T,\\ &\Upsilon_{k+1} \triangleq E\left[-\left(\left(\mathbf{I} - \breve{\mathbf{D}}_{k+1}\mathbf{M}_{k+1}\right)\mathbf{e}_{k+1}\right)\left(\tilde{\mathbf{e}}_{k+1}^{\mathbf{Z}}\right)^T\right] = -\left(\mathbf{I} - \breve{\mathbf{D}}_{k+1}\mathbf{M}_{k+1}\right)\left(\tilde{\mathbf{P}}_k^{\mathbf{Ze}}\right)^T,\\ &\tilde{\mathbf{P}}_k^{\mathbf{Ze}} \triangleq E\left[\left(\tilde{\mathbf{e}}_{k+1}^{\mathbf{Z}}\right)\left(\mathbf{e}_{k+1}\right)^T\right] = \left(\mathbf{A}_k^*\hat{\mathbf{P}}_k^{\mathbf{Z}} + \mathbf{J}_{k+1}\hat{\mathbf{P}}_k^{\mathbf{ZW}^T} - \mathbf{G}_{k+1}\hat{\mathbf{P}}_k^{\mathbf{ZV}^T}\right)\Gamma_{k+1}^T + \mathbf{A}_k^*\hat{\mathbf{P}}_k^{\mathbf{ZW}}\breve{\mathbf{L}}_{k+1}^T + \mathbf{A}_k^*\hat{\mathbf{P}}_k^{\mathbf{ZV}} + \mathbf{J}_{k+1}\overline{\mathbf{Q}}_k\breve{\mathbf{L}}_{k+1}^T - \mathbf{G}_{k+1}\overline{\mathbf{R}}_{k+1}.\end{aligned} \tag{37}$$

Therefore, $\mathbf{K}_{k+1}$ is estimated with the minimum-variance condition by minimizing the trace of $\hat{\mathbf{P}}_{k+1}^{\mathbf{Z}}$. However, the nonsingular matrix Ψ_{k+1} leads to the solution of $\mathbf{K}_{k+1}$ not unique [19]. If the singular value decomposition (SVD) is performed on Ψ_{k+1}, and the row vector of $\mathbf{S}_{k+1}$ is the singular vector corresponding to the non-zero singular value of Ψ_{k+1}. Then, $\mathbf{S}_{k+1}\Psi_{k+1}\mathbf{S}_{k+1}^T$ is invertible and $\mathbf{K}_{k+1}$ is finally obtained:

$$\mathbf{K}_{k+1} = -\Upsilon_{k+1}^T\mathbf{S}_{k+1}^T\left(\mathbf{S}_{k+1}\boldsymbol{\Psi}_{k+1}\mathbf{S}_{k+1}^T\right)^{-1}\mathbf{S}_{k+1}. \tag{38}$$

2.2.4. Covariance Matrices Derivation. However, the covariance matrices $\hat{\mathbf{P}}_{k+1}^{\mathbf{ZW}}$ and $\hat{\mathbf{P}}_{k+1}^{\mathbf{ZV}}$ are still unknown. A recursive form for their expressions are derived with reference to the method by Maex et al. [31].

By defining the matrix $\breve{\mathbf{I}}_W \triangleq \begin{bmatrix}\mathbf{0}_{(N-1)n\times n} & \mathbf{I}_{(N-1)n}\\ \mathbf{0}_{n\times n} & \mathbf{0}_{n\times(N-1)n}\end{bmatrix}$ and $\bar{\mathbf{I}}_W \triangleq \begin{bmatrix}\mathbf{0}_{(N-1)n\times n} & \mathbf{0}_{(N-1)n\times n}\\ \mathbf{0}_{n\times(N-1)n} & \mathbf{I}_n\end{bmatrix}$,

$$\mathbf{W}_{k+2} = \breve{\mathbf{I}}_W\mathbf{W}_{k+1} + \bar{\mathbf{I}}_W\mathbf{W}_{k+2}, \tag{39}$$

and a similar form can be established for the $\mathbf{V}_{k+2}$ with the similar definitions of $\breve{\mathbf{I}}_V$ and $\bar{\mathbf{I}}_V$.

Finally, the covariance matrices $\hat{\mathbf{P}}_{k+1}^{\mathbf{ZW}}$ and $\hat{\mathbf{P}}_{k+1}^{\mathbf{ZV}}$ are obtained based on equations (33) and (39) as:

$$\begin{aligned}\widehat{\mathbf{P}}_{k+1}^{\mathbf{ZW}} &= E\left[\left(\widehat{\mathbf{A}}_{k+1}\widehat{\mathbf{e}}_k^{\mathbf{Z}} + \widehat{\mathbf{J}}_{k+1}\mathbf{W}_{k+1} + \widehat{\mathbf{G}}_{k+1}\mathbf{V}_{k+1}\right)\left(\breve{\mathbf{I}}_W\mathbf{W}_{k+1} + \overline{\mathbf{I}}_W\mathbf{W}_{k+2}\right)^T\right] = \widehat{\mathbf{A}}_{k+1}\widehat{\mathbf{P}}_k^{\mathbf{ZW}}\breve{\mathbf{I}}_W^T + \widehat{\mathbf{J}}_{k+1}\overline{\mathbf{Q}}_{k+1}\breve{\mathbf{I}}_W^T,\\ \widehat{\mathbf{P}}_{k+1}^{\mathbf{ZV}} &= E\left[\left(\widehat{\mathbf{A}}_{k+1}\widehat{\mathbf{e}}_k^{\mathbf{Z}} + \widehat{\mathbf{J}}_{k+1}\mathbf{W}_{k+1} + \widehat{\mathbf{G}}_{k+1}\mathbf{V}_{k+1}\right)\left(\breve{\mathbf{I}}_V\mathbf{V}_{k+1} + \overline{\mathbf{I}}_V\mathbf{V}_{k+2}\right)^T\right] = \widehat{\mathbf{A}}_{k+1}\widehat{\mathbf{P}}_k^{\mathbf{ZV}}\breve{\mathbf{I}}_V^T + \widehat{\mathbf{G}}_{k+1}\overline{\mathbf{R}}_{k+1}\breve{\mathbf{I}}_V^T.\end{aligned} \tag{40}$$

3. Numerical Investigation

3.1. Numerical Model. To show the tolerance to measurement noises and efficiency of the proposed method, a six-storyshear-type building is adopted as the numerical validation model. The structural parameters are selected as: each mass $m_i = 100\text{kg}$, inter-story stiffness $k_i = 1000\text{kN/}m\,(i = 1, 2, \ldots, 6)$, and Rayleigh damping is assumed with the coefficient $\alpha = 1.0795\ \text{s}^{-1}, \beta = 6.3139 \times 10^{-4}$ s. The structure is excited by the El-Centro N-S earthquake with a peak ground acceleration (PGA) = 0.1 g. In this numerical model, the observed response data are inter-story displacement of all stories. All the used response data are polluted by Gauss-white noises with 10% root-mean-square (RMS), to show the tolerance to measurement noises of the proposed smoothing EKF-UI-WDF.

3.2. Identification of Unknown Seismic Input. As shown in Figure 1, the identification results under the conditions of one step delayed ($N = 1$) and five steps delayed ($N = 5$) are given in Figures 1(a) and 1(b) respectively. It can be seen from Figure 1(a) that the seismic acceleration identified by the traditional approach results in an obvious error, as the estimated unknown input is sensitive to measurement noise. On the other hand, the estimation of unknown input by the proposed has been greatly improved as shown in Figure 1(b). The main reason is that more information increases make the identification of unknown input more accurate. Figure 1(b) shows the identified seismic acceleration with 5 steps delayed, and the real value is tracked well.

In addition, it is discussed the effect of time delay to exchange for the improvement of identification. Figure 2 shows the relationship between the number of delayed time steps and the error covariance of the estimated unknown input. As the number of delayed steps increases, the error tends to be stable, which indicates that the improvement effect is finite and only a certain number of delayed steps (five steps in this case) has a very significant effect to measurement noises.

3.3. Identification of Structural States. Since the structural displacement response has been monitored, the identified velocity, taking the 1st story as an example, is selected to validate the proposed method for the identification of structural states. From Figure 3, it is known that the proposed method also plays a significant role in improving the state identification effect. When structural displacement observations are polluted by noises, there are many "burrs" in the identification result in Figure 3(a), However, these "burrs" are greatly reduced when five steps delayed is adopted in Figure 3(b).

Similarly, Figure 4 shows the estimated velocity error-reduction using different delayed steps. With five steps delayed, the improvement of the identification effect tends to be stable.

3.4. Identification of Structural Parameters. It is of great significance to identify structural parameters. In this subsection, the proposed smoothing EKF-UI-WDF is used to identify structural stiffness parameters. From Figure 5, it is noted that when the number of delayed steps increases, the identified parameters converge fast to the true value, in which the initial values of structural parameteres are selcted as 1.2 MN/m based on engineering experience. However, the resuctsive identifition of structural parameters may be disconvenrgenced if the initial values are set far away from their true values.

4. Real-World Application

4.1. A Brief Introduction to the Burbank Building. The identification of the six-story commercial building (Burbank building) in Burbank, California, USA (Figure 6) is investigated as a real-world application. The building built in 1976 is a steel structure building. The lateral loads are mainly carried by the perimeter frame, and the internal frame structure carries the vertical loads. So the analyzed structural system under the earthquake excitation is the perimeter frame structure, and the Burbank building can be simplified into a two-dimensionalsix-storysix-bay plane frame model as shown in Figure 7. More details of the Burbank building can be found in reference [32].

4.2. Model Updating Using EKF Method. Before the system identification of the Burbank building, model updating is used to know the real value of the structural parameters, especially the structural stiffness. Therefore, this subsection firstly updates the model based on the response data and seismic data recorded by the Center for Engineering Strong Motion Data (CESMD). The Burbank building was excited by the Sierra Madre earthquake in 1991. The sensors in the building (Figure 8) recorded the absolute acceleration response data. Because the seismic energy is low and the structure did not enter the nonlinear stage, the data can be used for model updating. In addition, only the first two natural frequencies of the structure can be identified, so it is more accurate to use time-domain data for model updating [38].

The EKF method is used for model updating using the horizontal absolute acceleration responses of the 1st and 6th

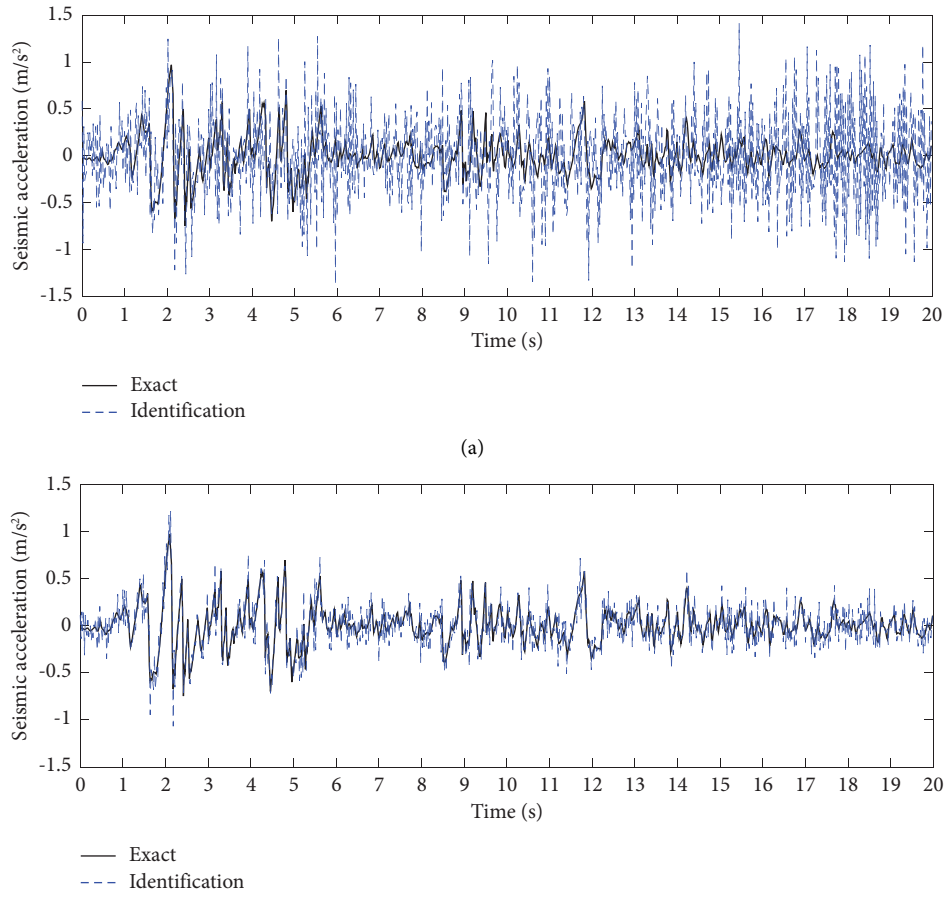

Figure 1: Identification of unknown seismic input. (a) EKF-UI-WDF ($N = 1$). (b) Smoothing EKF-UI-WDF ($N = 5$).

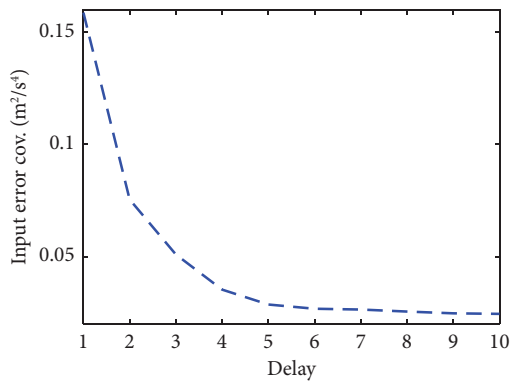

Figure 2: Effect of delayed steps on identified input error covariance.

stories, and the 1991 Sierra Madre earthquake is used as known seismic input. The accuracy of model updating is checked by comparing the 2nd story horizontal acceleration responses.

4.2.1. Updating Beam and Column Stiffness. The six-storysix-bay plane frame model in Figure 7 has 36 beam and 42 column elements, among which the sixth bay beam is shear connected to the side column, and the rest are fixed. Therefore, there are 54 DOFs, including 6 horizontal DOFs and 48 rotational DOFs, when axial deformations of elements are ignored.

A major purpose of model updating is to determine the actual values of the structural parameters. The design information of beam and column components of each story can be obtained from the design information in Table 1. The ASTM A36 steel is used for all beam and column elements with the yield strength of 255 MPa [39]. Based on the design information, the design value of the stiffness of the beam and column elements in each story can be calculated and taken as the initial value of the EKF method. Table 2 shows the comparison of beam and column stiffness of each story after updating. The updated results obtained in Table 2 are used later as compared values for the identification in this case study.

4.2.2. Updating Structural Damping. The first two damping ratios identified by the Eigensystem Realization Algorithm (ERA) are 3.37% and 6.61% [40]. Herein, Rayleigh damping with the damping coefficients before updating as $\alpha^0 = 0.0920\text{s}^{-1}$ and $\beta^0 = 0.0098$ s is adopted. These two

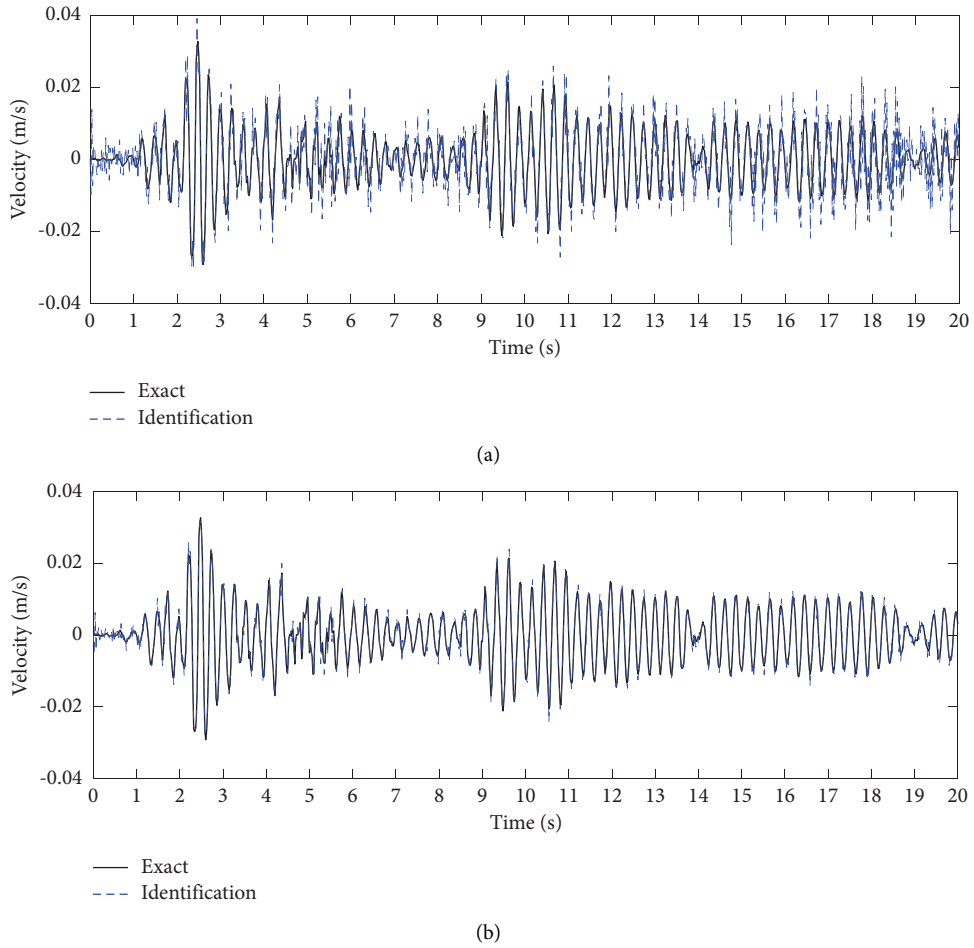

FIGURE 3: Identification of velocity response. (a) EKF-UI-WDF ($N = 1$). (b) Smoothing EKF-UI-WDF ($N = 5$).

values are used as the initial values of damping coefficients in the EKF method, and the updated values are $\alpha^{\mathrm{EKF}} = 0.0500\ \mathrm{s}^{-1}$ and $\beta^{\mathrm{EKF}} = 0.0229$ s.

4.2.3. Comparison of the 2nd Story Accelerations. To reflect the effect of model updating, the comparison of the 2nd story horizontal absolute accelerations is shown in Figure 9, in which Figure 9(a) shows the acceleration before model updating while Figure 9(b) shows the acceleration after model updating by the EKF method. The compared acceleration is the horizontal absolute acceleration, however, the directly obtained states from EKF are relative to the ground. As can be seen from Figure 9, the time-domain history of the 2nd story horizontal absolute acceleration response after model updating has a better agreement with the monitored data than that before model updating, which proves the accuracy of model updating through the EKF method.

4.3. Identification of Unknown Seismic Input and Structural System. This subsection will validate the effectiveness of the smoothing EKF-UI-WDF method in unknown seismic input and Burbank building system identification. The 1991 Sierra Madre earthquake is also selected here as the unknown seismic input, and the used observations are the 2nd and 6th story horizontal absolute acceleration monitored by the sensors shown in Figure 7. The identified states and parameters are compared with those from the EKF method. And the satisfactory identification is obtained as follows when the 10 steps are delayed ($N = 10$).

4.3.1. Identification of Seismic Input. Figure 10 shows the identification of the ground acceleration. In the case of 10 steps delayed, the overall identified values are in good agreement. Considering the complexity of this practical structural engineering, the identified result is acceptable.

4.3.2. Identification of Displacement. Figures 11(a) and 11(b) show the identification of horizontal relative displacement of the 2nd and 6th story respectively. Since there are no monitored displacement response data, it is compared with the identified displacement by the EKF method. The identification results are in a reasonable range and can be further used in structural condition assessment.

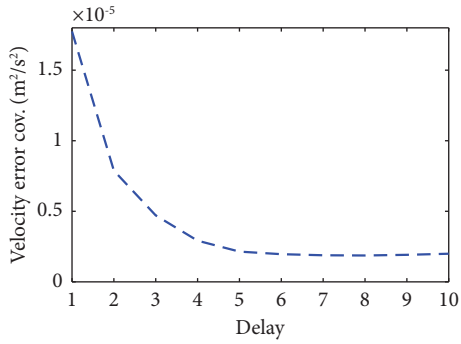

Figure 4: Effect of delayed steps on identified velocity error covariance.

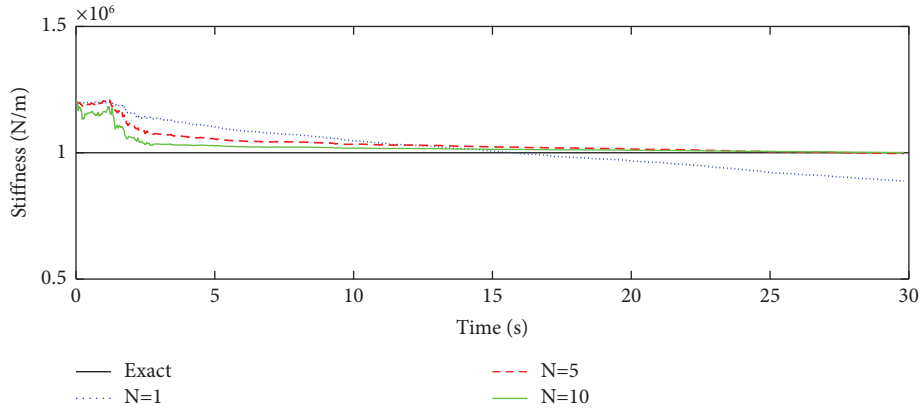

Figure 5: Identification of the 5th story stiffness with different delayed steps.

Figure 6: Exterior elevation of Burbank building.

4.3.3. Identification of Structural Stiffness. The updated structural stiffness k^{EKF} is taken as the comparative reference herein. Figures 12(a) and 12(b) show the identified stiffness of the 5th and 6th story columns respectively. The identified parameter values converge quickly, which verifies the effectiveness of the proposed method.

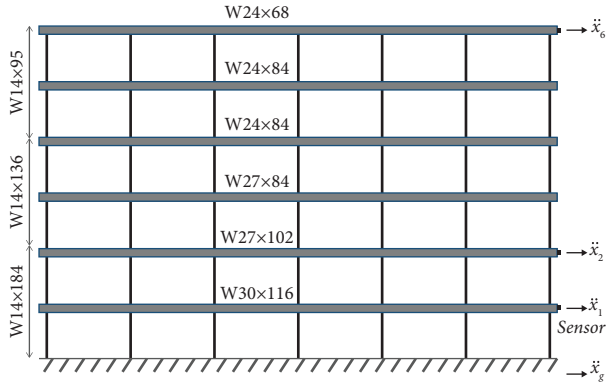

Figure 7: Six-storysix-bay plane frame [3].

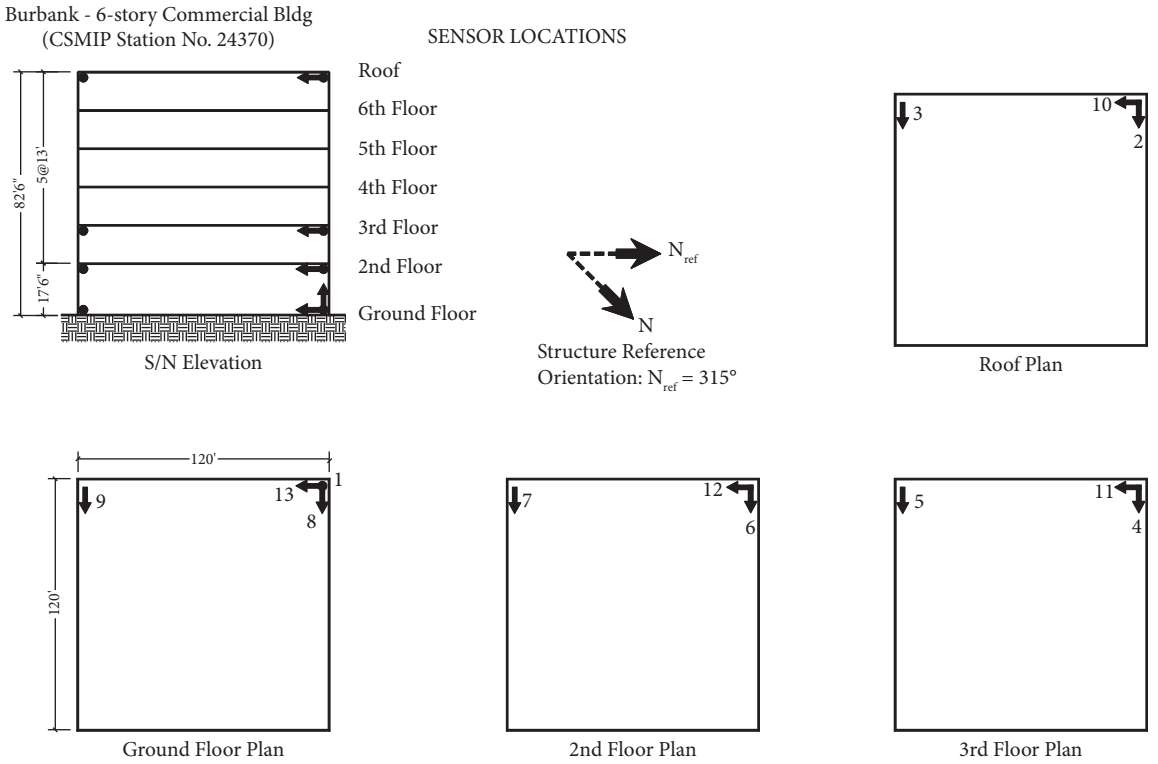

Figure 8: Sensor locations. (Figures 6 and 8 are from https://www.strongmotioncenter.org/cgi-bin/CESMD/stationhtml.pl?stationID=CE24370&network=CGS).

Table 1: Design information of beam and column.

Elements	Designation	Section area (m^2)	Elastic property ($10^{-8}m^{-4}$)	Elemental length (m)
B1	W30 × 116	22064.47	205202.09	6.10
B2	W27 × 102	19354.80	150675.78	6.10
B3	W27 × 84	15999.97	118625.96	6.10
B4	W24 × 84	15935.45	98646.85	6.10
B5	W24 × 84	15935.45	98646.85	6.10
B6	W24 × 68	12967.72	76170.35	6.10
C1	W14 × 184	34937.31	94166.24	5.18
C2	W14 × 184	34937.31	94166.24	3.96
C3	W14 × 136	25784.90	65764.57	3.96
C4	W14 × 136	25784.90	65764.57	3.96
C5	W14 × 95	18028.64	44148.28	3.96
C6	W14 × 95	18028.64	44148.28	3.96

Note. "B1" represents all beams of the 1st story and "C1" represents all columns of the 1st story.

Table 2: Stiffness of beam and column.

Elements	Design value k^0 (N/m)	Updated value k^{EKF} (N/m)
B1	85781	85445
B2	62987	64127
B3	49590	52071
B4	41238	38237
B5	41238	42326
B6	31842	32043
C1	46356	46241
C2	60637	60611
C3	42348	42541
C4	42348	42476
C5	28429	28891
C6	28429	28607

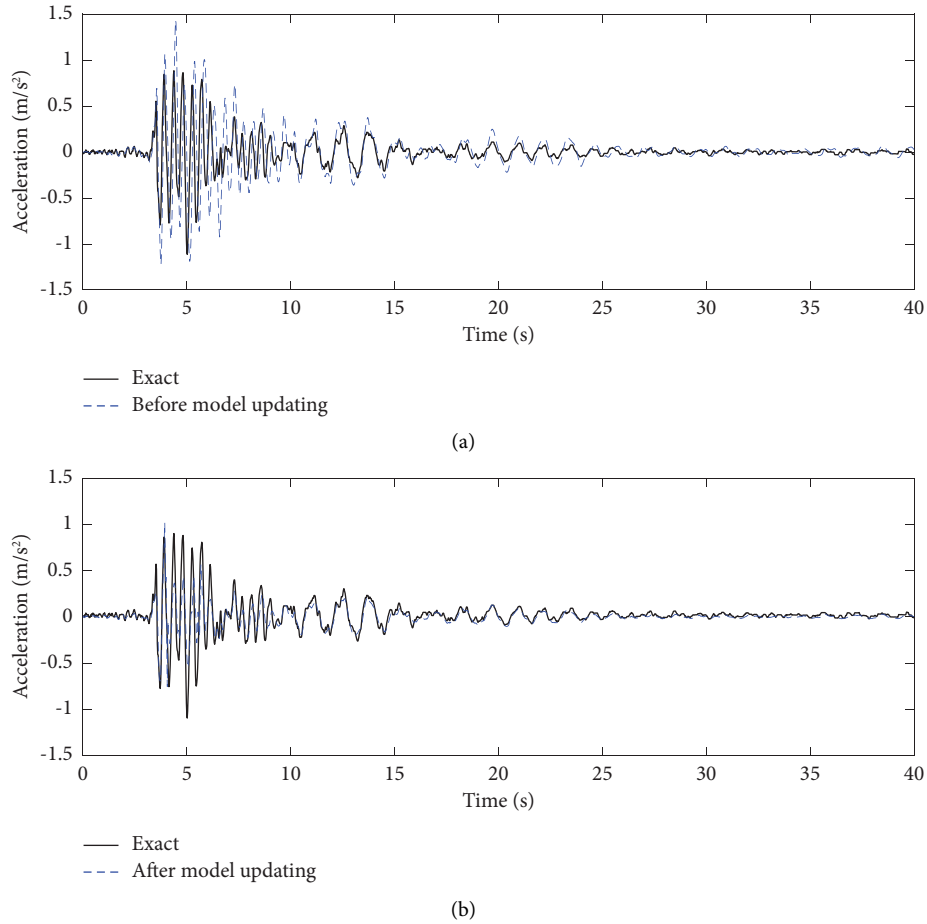

Figure 9: Comparison of the 2nd story accelerations before and after model updating. (a) Before model updating. (b) After model updating.

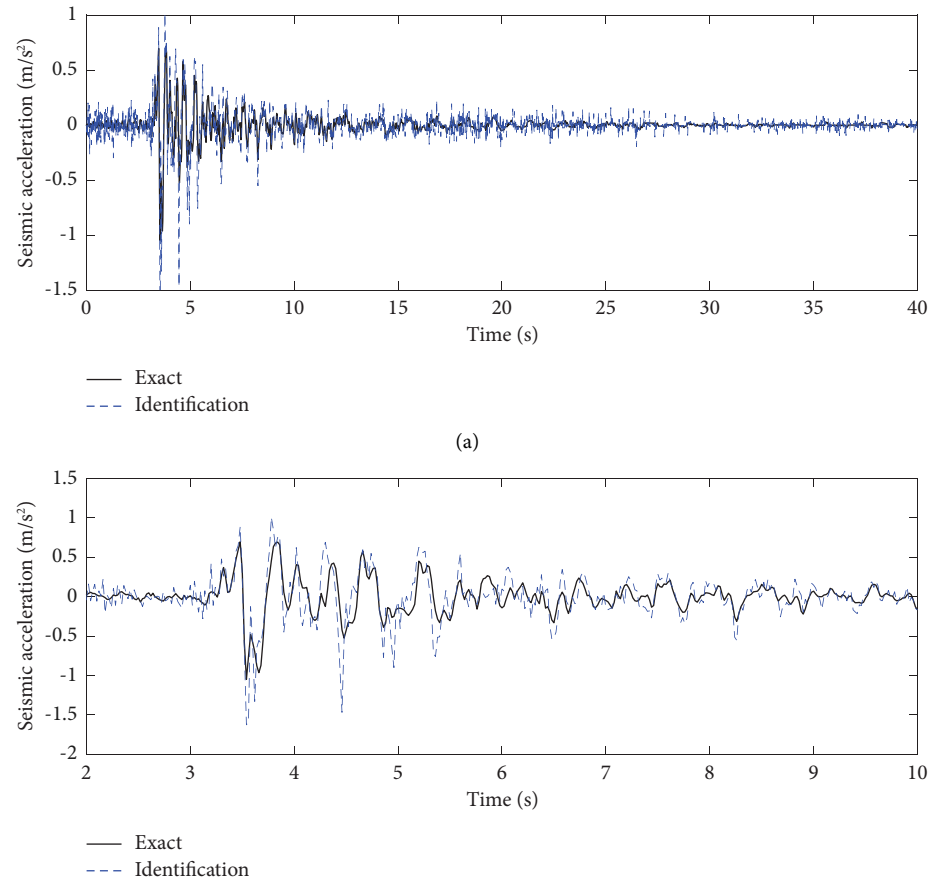

Figure 10: Identification of seismic acceleration (1991 sierra madre earthquake). (a) Identification of seismic input (0–40 s). (b) Identification of seismic input (2–10 s).

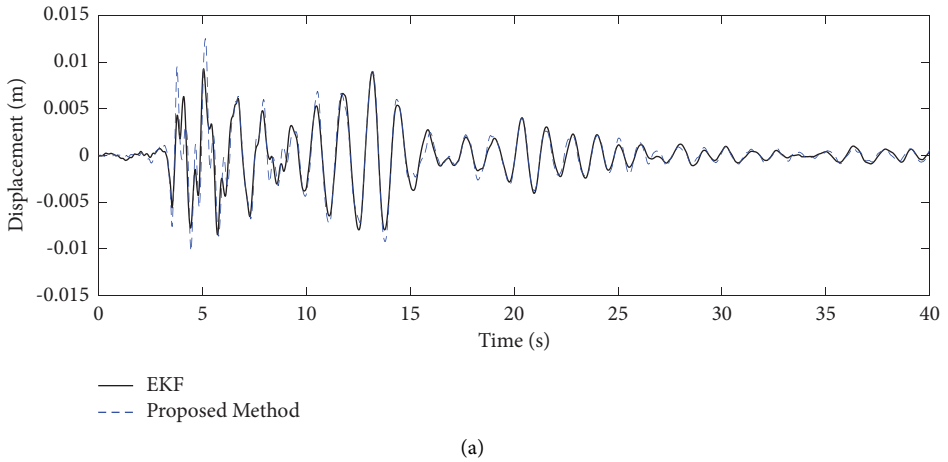

Figure 11: Continued.

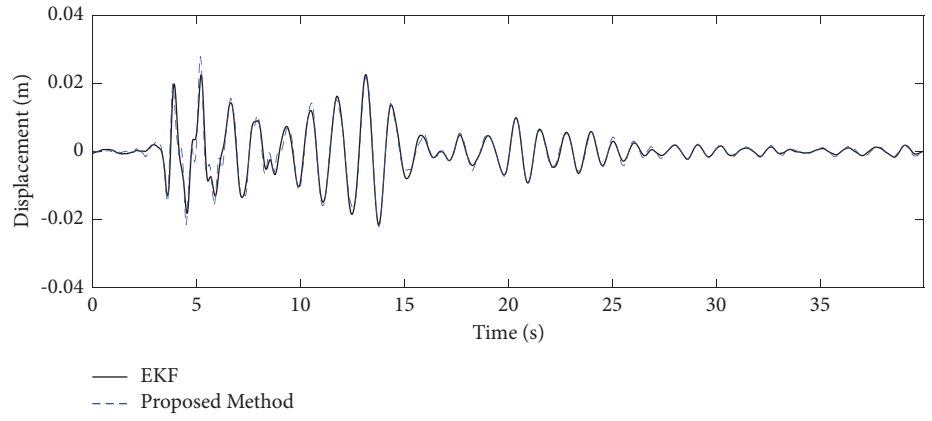

(b)

FIGURE 11: Identification of horizontal relative displacement. (a) 2nd story displacement. (b) 6th story displacement.

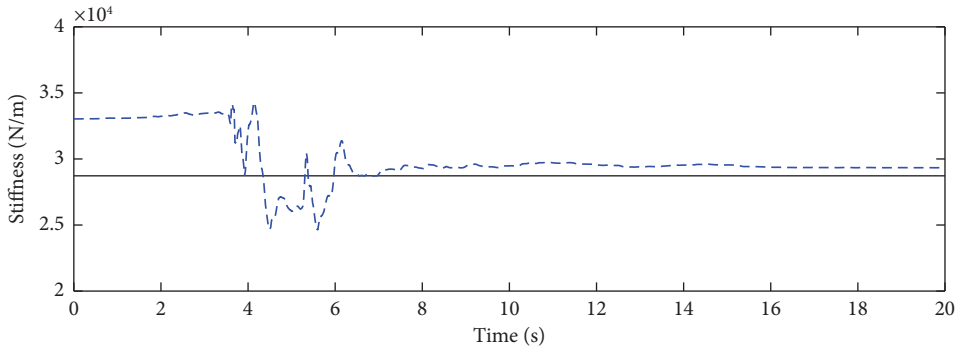

(a)

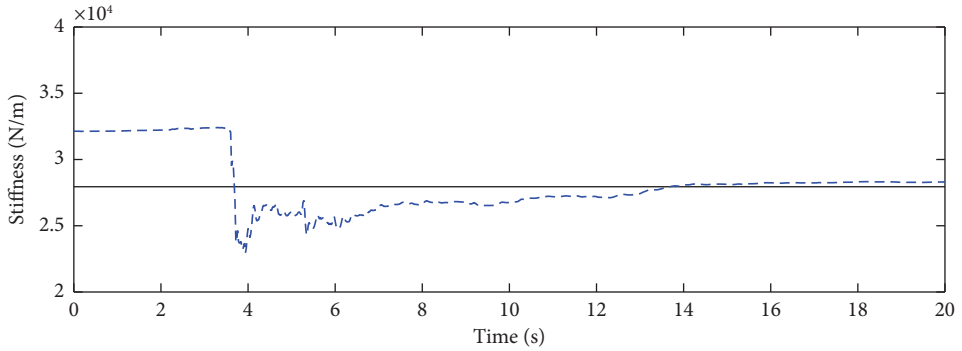

(b)

FIGURE 12: Identification of structural stiffness. (a) Stiffness of the 5th story column. (b) Stiffness of the 6th story column.

5. Conclusions

Most of the current identification methods are not suitable for the simultaneous identification of structural systems and unknown seismic inputs using partial observations of absolute acceleration response of structures, and the identification results are greatly affected by the measurement noises. In this paper, a new method namely smoothing EKF-UI-WDF is proposed to solve the problem. This method can not only achieve the simultaneous identification of structural states, parameters of the

structural system, and unknown seismic inputs without direct feedthrough but also reduce the influence of measurement noise on the identification results.

The effectiveness and practicability of the proposed method are verified by a numerical model case and a practical engineering case. In the numerical model case, monitored dynamic displacement response polluted by a quite high level of noise is used. The proposed method gives satisfactory identification results and shows tolerance to measurement noises. The real-world application case is based on the Burbank building in California, USA. Using the measured absolute acceleration response of some floors in the 1991 Sierra Madre earthquake, the unknown seismic input together with structural states and parameters are identified by the proposed method. The identification results show the applicability of the proposed method in practical engineering.

However, the presented smoothing EKF-UI-WDF in this paper is only suitable for the identification of time-invariant structure systems. The extension work for the identification of time-variant structure systems is undertaken by the authors.

Data Availability

The data used in this study are available from the corresponding author upon reasonable request.

Conflicts of Interest

The authors declare that they have no conflicts of interest.

Acknowledgments

The research in this paper is financially supported by the National Natural Science Foundation of China via the grant no. 52178304.

References

[1] X. Z. Lu, Q. L. Cheng, Z. Xu, Y. J. Xu, and C. J. Sun, "Real-timecity-scaletime-history analysis and its application in resilience-oriented earthquake emergency responses," *Applied Sciences*, vol. 9, no. 17, p. 3497, 2019.

[2] X. Z. Lu, Y. J. Xu, Y. Tian, B. Cetiner, and E. Taciroglu, "A deep learning approach to rapid regional post-event seismic damage assessment using time-frequency distributions of ground motions," *Earthquake Engineering and Structural Dynamics*, vol. 50, no. 6, pp. 1612–1627, 2021.

[3] S. A. Taher, J. Li, and H. Z. Fang, "Earthquake input and state estimation for buildings using absolute floor accelerations," *Earthquake Engineering and Structural Dynamics*, vol. 50, no. 4, pp. 1020–1042, 2021.

[4] X. Zhi-Qian, P. Jian-Wen, W. Jin-Ting, and C. Fu-Dong, "Improved approach for vibration-based structural health monitoring of arch dams during seismic events and normal operation," *Structural Control and Health Monitoring*, vol. 29, no. 7, 2022.

[5] K. Q. Xu and A. Mita, "Estimation of maximum drift of multi-degree-of-freedom shear structures with unknown parameters using only one accelerometer," *Structural Control and Health Monitoring*, vol. 28, no. 9, 2021.

[6] Y. Q. Ni, Y. Xia, W. Y. Liao, and J. M. Ko, "Technology innovation in developing the structural health monitoring system for Guangzhou New TV Tower," *Structural Control and Health Monitoring*, vol. 16, no. 1, pp. 73–98, 2009.

[7] Y. Niu, C. P. Fritzen, H. Jung, I. Buethe, Y. Q. Ni, and Y. W. Wang, "Online simultaneous reconstruction of wind load and structural responses-theory and application to Canton Tower," *Computer-Aided Civil and Infrastructure Engineering*, vol. 30, no. 8, pp. 666–681, 2015.

[8] S. F. Ghahari, F. Abazarsa, H. Ebrahimian, and E. Taciroglu, "Output-only model updating of adjacent buildings from sparse seismic response records and identification of their common excitation," *Structural Control and Health Monitoring*, vol. 27, no. 9, 2020.

[9] X. W. Ye, Y. Ding, and H. P. Wan, "Probabilistic forecast of wind speed based on Bayesian emulator using monitoring data," *Structural Control and Health Monitoring*, vol. 28, no. 1, 2021.

[10] J. L. Liu, A. H. Yu, C. M. Chang, W. X. Ren, and J. Zhang, "A new physical parameter identification method for shear frame structures under limited inputs and outputs," *Advances in Structural Engineering*, vol. 24, no. 4, pp. 667–679, 2021.

[11] R. E. Kalman, "A new approach to linear filtering and prediction problems," *Journal of Basic Engineering*, vol. 82, no. 1, pp. 35–45, 1960.

[12] J. N. Yang, S. W. Pan, and H. Huang, "An adaptive extended Kalman filter for structural damage identifications II: unknown inputs," *Structural Control and Health Monitoring*, vol. 14, no. 3, pp. 497–521, 2007.

[13] B. Xu, J. He, R. Rovekamp, and S. J. Dyke, "Structural parameters and dynamic loading identification from incomplete measurements: approach and validation," *Mechanical Systems and Signal Processing*, vol. 28, pp. 244–257, 2012.

[14] Y. Lei, Y. Q. Jiang, and Z. Q. Xu, "Structural damage detection with limited input and output measurement signals," *Mechanical Systems and Signal Processing*, vol. 28, pp. 229–243, 2012.

[15] Y. Lei, M. Y. He, C. Liu, and S. Z. Lin, "Identification of tall shear buildings under unknown seismic excitation with limited output measurements," *Advances in Structural Engineering*, vol. 16, no. 11, pp. 1839–1849, 2013.

[16] Y. Lei, C. Liu, and L. J. Liu, "Identification of multistory shear buildings under unknown earthquake excitation using partial output measurements: numerical and experimental studies," *Structural Control and Health Monitoring*, vol. 21, pp. 774–783, 2014.

[17] L. J. Liu, Y. Su, J. J. Zhu, and Y. Lei, "Data fusion based EKF-UI for real-time simultaneous identification of structural systems and unknown external inputs," *Measurement*, vol. 88, pp. 456–467, 2016.

[18] K. Maes, A. W. Smyth, G. De Roeck, and G. Lombaert, "Joint input-state estimation in structural dynamics," *Mechanical Systems and Signal Processing*, vol. 70-71, pp. 445–466, 2016.

[19] K. V. Yuen and K. Huang, "Real-time substructural identification by boundary force modeling," *Structural Control and Health Monitoring*, vol. 25, no. 5, 2018.

[20] K. Huang and K. V. Yuen, "Online dual-rate decentralized structural identification for wireless sensor networks," *Structural Control and Health Monitoring*, vol. 26, no. 11, p. e2453, 2019.

[21] K. Huang, K. V. Yuen, and L. Wang, "Real-time simultaneous input-state-parameter estimation with modulated colored noise excitation," *Mechanical Systems and Signal Processing*, vol. 165, Article ID 108378, 2022.

[22] S. Gillijns and B. De Moor, "Unbiased minimum-variance input and state estimation for linear discrete-time systems," *Automatica*, vol. 43, no. 1, pp. 111–116, 2007.

[23] S. W. Pan, H. Y. Su, H. Wang, J. Chu, and R. Q. Lu, "Input and state estimation for linear systems: a least squares estimation approach," in *Proceedings of the 2009 7th Asian Control Conference*, Hong Kong, China, August 2009.

[24] Z. M. Wan, T. Wang, L. Li, and Z. C. Xu, "A novel coupled state/input/parameter identification method for linear structural systems," *Shock and Vibration*, vol. 2018, Article ID 7691721, 15 pages, 2018.

[25] S. W. Pan, H. Y. Su, J. Chu, and H. Wang, "Applying a novel extended Kalman filter to missile–target interception with APN guidance law: a benchmark case study," *Control Engineering Practice*, vol. 18, no. 2, pp. 159–167, 2010.

[26] J. S. Huang, X. Z. Li, F. B. Zhang, and Y. Lei, "Identification of joint structural state and earthquake input based on a generalized Kalman filter with unknown input," *Mechanical Systems and Signal Processing*, vol. 151, no. 9, Article ID 107362, 2021.

[27] Y. Lei, J. B. Lu, and J. S. Huang, "Synthesize identification and control for smart structures with time-varying parameters under unknown earthquake excitation," *Structural Control and Health Monitoring*, vol. 27, no. 4, 2020.

[28] K. Maes, S. Gillijns, and G. Lombaert, "A smoothing algorithm for joint input-state estimation in structural dynamics," *Mechanical Systems and Signal Processing*, vol. 98, pp. 292–309, 2018.

[29] D. M. Feng and M. Q. Feng, "Identification of structural stiffness and excitation forces in time domain using noncontact vision-based displacement measurement," *Journal of Sound and Vibration*, vol. 406, pp. 15–28, 2017.

[30] G. Yan, H. Sun, and O. Buyukozturk, "Impact load identification for composite structures using Bayesian regularization and unscented Kalman filter," *Structural Control and Health Monitoring*, vol. 24, no. 5, 2017.

[31] K. Maes, F. Karlsson, and G. Lombaert, "Tracking of inputs, states and parameters of linear structural dynamic systems," *Mechanical Systems and Signal Processing*, vol. 130, pp. 755–775, 2019.

[32] U. Lagerblad, H. Wentzel, and A. Kulachenko, "Dynamic response identification based on state estimation and operational modal analysis," *Mechanical Systems and Signal Processing*, vol. 129, pp. 37–53, 2019.

[33] U. Lagerblad, H. Wentzel, and A. Kulachenko, "Study of a fixed-lag Kalman smoother for input and state estimation in vibrating structures," *Inverse Problems in Science and Engineering*, vol. 29, no. 9, pp. 1260–1281, 2021.

[34] W. Feng, Q. F. Li, and Q. H. Lu, "Force localization and reconstruction based on a novel sparse Kalman filter," *Mechanical Systems and Signal Processing*, vol. 144, Article ID 106890, 2020.

[35] M. H. Ebrahimzadeh, A. Heidarpour, S. Eftekhar Azam, and M. Arashpour, "A Bayesian smoothing for input-state estimation of structural systems," *Computer-Aided Civil and Infrastructure Engineering*, vol. 37, no. 3, pp. 317–334, 2022.

[36] K. V. Yuen and S. C. Kuok, "Online updating and uncertainty quantification using nonstationary output-only measurement," *Mechanical Systems and Signal Processing*, vol. 66-67, pp. 62–77, 2016.

[37] K. V. Yuen, P. F. Liang, and S. C. Kuok, "Online estimation of noise parameters for Kalman filter," *Structural Engineering and Mechanics*, vol. 47, no. 3, pp. 361–381, 2013.

[38] J. C. Anderson, *Seismic Performance of an Instrumented Six-story Steel Building*, Earthquake Engineering Research Center, University of California at Berkeley, Berkeley, California, 1991.

[39] E. D'Amore and A. Astaneh-Asl, "Case study of expected seismic performance of an instrumented steel moment frame building," in *Proceedings of the Conference on Seismic Engineering Conference*, Calabria, Italy, July 2008.

[40] S. L. Lin, J. Li, A. S. Elnashai, and B. F. Spencer Jr, "NEES integrated seismic risk assessment framework (NISRAF)," *Soil Dynamics and Earthquake Engineering*, vol. 42, pp. 219–228, 2012.